

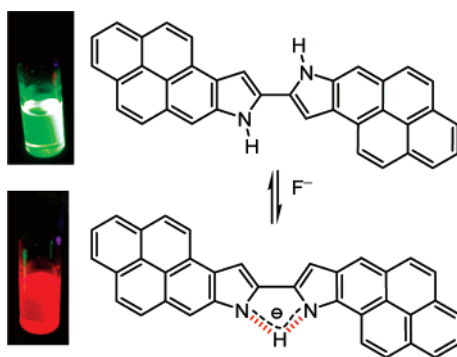
Pyreno[2,1-*b*]pyrrole and Bis(pyreno[2,1-*b*]pyrrole) as Selective Chemosensors of Fluoride Ion: A Mechanistic Study

Chia-I Lin,[†] Srinivasan Selvi,[†] Jim-Min Fang,^{*,†,‡} Pi-Tai Chou,^{*,†} Chin-Hung Lai, and Yi-Ming Cheng

Department of Chemistry, National Taiwan University, Taipei 106, Taiwan, and The Genomics Research Center, Academia Sinica, Taipei 115, Taiwan

jmfang@ntu.edu.tw; chop@ntu.edu.tw

Received January 29, 2007



Pyreno[2,1-*b*]pyrrole and its dimeric derivative display excellent selectivity and sensitivity for detection of fluoride ion, in comparison with chloride, bromide, iodide, acetate, dihydrogen phosphate, hydrogen sulfate, perchlorate, nitrate, and thiocyanate ions. The hydrogen bonding with fluoride ion, both in formation and in subsequent dissociation, provides remarkable colorimetric and fluorescent changes in the visible region that are advantageous for real-time and on-site application. Detailed NMR and dynamic fluorescence spectroscopic analyses establish the associated mechanism.

Introduction

Paramount interest has been laid over the past decade on the development of synthetic anion sensors capable of converting the binding event into readable signal output through optical, electrochemical, and magnetic resonance responses.¹ In many circumstances, the sensing of anions is indispensable in biological, environmental, and industrial research.² For example, fluoride is a common ingredient in anesthetics, hypnotics,

psychiatric drugs, rat and cockroach poisons, and military nerve gases,³ and is a contaminant in drinking water. Excess fluoride exposure may cause collagen breakdown, bone disorders, thyroid activity depression, and immune system disruption.³ In view of the above properties, detection of fluoride with use of simple preparation and minimal instrumental assistance is desirable toward practical applications.

The neutral type anion sensors^{1,4} usually consist of hydrogen-bonding units such as pyrrole, urea, amide, amine, phenol, and Lewis acid in the recognition sites. On the other hand, the positively charged sensors^{1,5} can generally be ammonium, guanidinium, quinolinium and protonated quinoxaline salts, and metal complexes to provide electrostatic interactions with the guest anions. Recently, the sensors made by immobilization of

[†] National Taiwan University.

[‡] The Genomics Research Center.

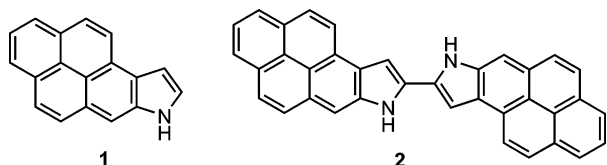
(1) (a) Schmidtchen, F. P.; Berger, M. *Chem. Rev.* **1997**, *97*, 1609–1646. (b) Beer, P. D.; Gale, P. A. *Angew. Chem., Int. Ed.* **2001**, *40*, 486–516. (c) Suksai, C.; Tuntulani, T. *Chem. Soc. Rev.* **2003**, *32*, 192–202. (d) Martínez-Máñez, R.; Sancenón, F. *Chem. Rev.* **2003**, *103*, 4419–4476. (e) Martínez-Máñez, R.; Sancenón, F. *J. Fluoresc.* **2005**, *15*, 267–285. (f) Gunnlaugsson, T.; Glynn, M.; Tocchi, G. M.; Kruger, P. E.; Pfeffer, F. M. *Coord. Chem. Rev.* **2006**, *250*, 3094–3117.

(2) (a) *Comprehensive Supramolecular Chemistry*; Atwood, J. L., Davies, J. E., MacNicol, D. D., Vögtle, F., Reinhoudt, D. N., Lehn, J.-M., Eds.; Pergamon-Elsevier Science: Oxford, UK, 1996. (b) *Supramolecular Chemistry of Anions*; Bianchi, A., Bowman-James, K., García-España, E., Eds.; Wiley-VCH: New York, 1997.

(3) (a) Waldbott, G. *Clin. Toxicol.* **1981**, *18*, 531–541. (b) Matuso, S.; Kiyomiya, K.-i.; Kurebe, M. *Arch. Toxicol.* **1998**, *72*, 798–806. (c) Zhang, S.-W.; Swager, T. M. *J. Am. Chem. Soc.* **2003**, *125*, 3420–3421. (d) Riggs, B. L. *Bone Miner. Res.* **1984**, *366–393*. (e) Laisalmi, M.; Kokki, H.; Soikkeli, A.; Markkanen, H.; Yli-Hankala, A.; Rosenberg, P.; Lindgren, L. *Acta Anaesthesiol. Scand.* **2006**, *50*, 982–987.

amides and metal complexes on nanoparticles⁶ have shown improved sensitivity toward anions.

The pyrrole-based anion probes, developed by several research groups,⁷ show excellent stability over a wide range of pH 3–10. To raise the detection sensitivity, the pyrrole units can be incorporated into a conjugated system for colorimetric detection⁷ or linked to fluorophores⁸ such as naphthalene, anthracene, pyrene, dansyl, fluorescein, and rhodamine that can involve various sensing mechanisms for signal transduction. We demonstrate herein the intrinsic type anion sensors, pyreno[2,1-*b*]pyrrole (**1**) and 2,2-bis(pyreno[2,1-*b*]pyrrole) (**2**), which contain the pyrrole recognition unit fused with the aromatic fluorophore.⁹



Results and Discussion

Compounds 1 and 2 with Fluoride Ion in DMSO. The idea to render the in-built pyrene moiety is in that the eventual charge transfer would exhibit signal output in the visible region due to the elongation of the π electron conjugation. We had earlier explored that **1** and **2** are indeed highly fluorescent compounds, having quantum yields, Φ_F , of 0.95 and 0.50, respectively, in EtOAc.⁹ We thus prepared a stock solution of **1** in DMSO (2×10^{-4} M), and carefully screened its binding ability with

(4) For reviews, see: (a) Sessler, J. L.; Camiolo, S.; Gale, P. A. *Coord. Chem. Rev.* **2003**, *240*, 17–55. (b) Vázquez, M.; Fabbri, L.; Taglietti, A.; Pedrido, R. M.; González-Noya, A. M.; Bermejo, M. R. *Angew. Chem., Int. Ed.* **2004**, *43*, 1962–1965. (c) Bondy, C. R.; Loeb, S. J. *Coord. Chem. Rev.* **2003**, *240*, 77–99. (d) Choi, K.; Hamilton, A. D. *Coord. Chem. Rev.* **2003**, *240*, 101–110. (e) Kubo, Y.; Yamamoto, M.; Ikeda, M.; Takeuchi, M.; Shinkai, S.; Yamaguchi, S.; Tamao, K. *Angew. Chem., Int. Ed.* **2003**, *42*, 2036–2040. For recent examples, see: (f) Kim, S. K.; Bok, J. H.; Bartsch, R. A.; Lee, J. Y.; Kim, J. S. *Org. Lett.* **2005**, *7*, 4839–4842. (g) Koskela, S. J. M.; Fyles, T. M.; James, T. D. *Chem. Commun.* **2005**, 945–947. (h) Wu, J.-S.; Zhou, J.-H.; Wang, P.-F.; Zhang, X.-H.; Wu, S.-K. *Org. Lett.* **2005**, *7*, 2133–2136. (i) Ren, J.; Zhao, X.-L.; Wang, Q.-C.; Ku, C.-F.; Qu, D.-H.; Chang, C.-P.; Tian, H. *Dyes Pigm.* **2005**, *64*, 193–200. (j) Cho, E. J.; Ryu, B. J.; Lee, Y. J.; Nam, K. C. *Org. Lett.* **2005**, *7*, 2607–2609. (k) Badugua, R.; Lakowicz, J. R.; Geddes, C. D. *Sens. Actuators, B* **2005**, *104*, 103–110. (l) Ilioudis, C. A.; Tocher, D. A.; Steed, J. W. *J. Am. Chem. Soc.* **2004**, *126*, 12395–12402. (m) Wen, Z.-C.; Jiang, Y.-B. *Tetrahedron* **2004**, *60*, 11109–11115. (n) Arimori, S.; Davidson, M. G.; Fyles, T. M.; Hibbert, T. G.; James, T. D.; Kociok-Koehn, G. I. *Chem. Commun.* **2004**, 1640–1641. (o) Xu, G.; Tarr, M. A. *Chem. Commun.* **2004**, 1050–1051. (p) Jimenez, D.; Martinez-Manez, R.; Sancenon, F.; Soto, J. *Tetrahedron Lett.* **2002**, *43*, 2823–2825. (q) DiCesare, N.; Lakowicz, J. R. *Anal. Biochem.* **2002**, *301*, 111–116. (r) Aldridge, S.; Bresner, C.; Fallis, I. A.; Coles, S. J.; Hursthouse, M. B. *Chem. Commun.* **2002**, 740–741. (s) Miyaji, H.; Sessler, J. L. *Angew. Chem., Int. Ed.* **2001**, *40*, 154–157.

(5) For reviews, see: (a) Best, M. D.; Tobey, S. L.; Anslin, E. V. *Coord. Chem. Rev.* **2003**, *240*, 3–15. (b) Llinares, J. M.; Powell, D.; Bowman-James, K. *Coord. Chem. Rev.* **2003**, *240*, 57–75. For recent examples, see: (c) Badugua, R.; Lakowicz, J. R.; Geddes, C. D. *Sens. Actuators, B* **2005**, *104*, 103–110. (d) Melaimi, M.; Gabbaie, F. P. *J. Am. Chem. Soc.* **2005**, *127*, 9680–9681. (e) Amendola, V.; Fabbri, L.; Monzani, E. *Chem. Eur. J.* **2004**, *10*, 76–82. (f) Badugua, R.; Lakowicz, J. R.; Geddes, C. D. *J. Fluoresc.* **2004**, *14*, 693–703. (g) Zhang, B.-g.; Cai, P.; Duan, C.-y.; Miao, R.; Zhu, L.-g.; Niitsu, T.; Inoue, H. *Chem. Commun.* **2004**, 2206–2207. (h) Mizukami, S.; Nagano, T.; Urano, Y.; Odani, A.; Kikuchi, K. *J. Am. Chem. Soc.* **2002**, *124*, 3920–3925. (i) Han, M. S.; Kim, D. H. *Angew. Chem., Int. Ed.* **2002**, *41*, 3809–3811.

(6) (a) Beer, P. D.; CORMODE, D. P.; Davis, J. J. *Chem. Commun.* **2004**, 414–415. (b) Labande, A.; Ruiz, J.; Astruc, D. *J. Am. Chem. Soc.* **2002**, *124*, 1782–1789. (c) Watanabe, S.; Sonobe, M.; Arai, M.; Tazume, Y.; Matsuo, T.; Nakamura, T.; Yoshida, K. *Chem. Commun.* **2002**, 2866–2867.

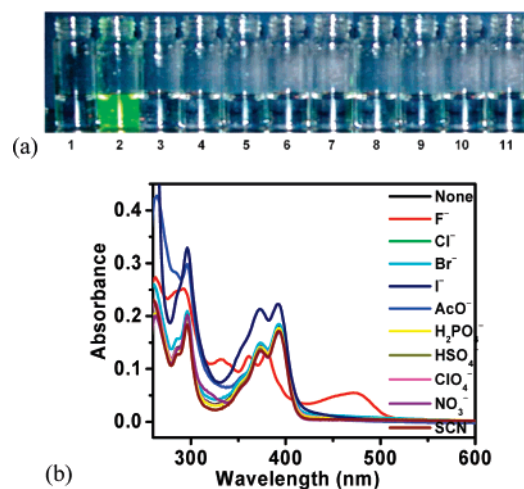


FIGURE 1. (a) Color change induced upon addition of anion (100 equiv as the Bu₄N⁺ salt) to receptor **1** (2×10^{-4} M in DMSO). From left to right: (1) no anion, (2) F⁻, (3) Cl⁻, (4) Br⁻, (5) I⁻, (6) AcO⁻, (7) H₂PO₄⁻, (8) HSO₄⁻, (9) ClO₄⁻, (10) NO₃⁻, and (11) SCN⁻. (b) Absorption spectral changes of receptor **1** (5×10^{-6} M) in DMSO in the presence of various anions (100 equiv).

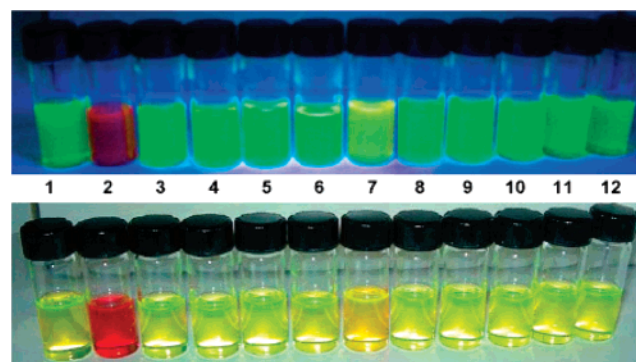


FIGURE 2. Color change induced upon addition of anions (100 equiv as the Bu₄N⁺ salt) to receptor **2** (1×10^{-4} M in DMSO): (top series) under irradiation with 364-nm light and (bottom series) under daylight. From left to right: (1) no anion, (2) F⁻, (3) Cl⁻, (4) Br⁻, (5) I⁻, (6) AcO⁻, (7) H₂PO₄⁻, (8) HSO₄⁻, (9) ClO₄⁻, (10) NO₃⁻, (11) SCN⁻, and (12) benzoate ion.

various anions (as the tetrabutylammonium salts). This system portrayed an excellent optical response toward fluoride ion (Figure 1a). The colorless solution of **1** turned grass-green upon addition of F⁻, whereas no naked-eye sensible color change occurred upon addition of other anions, including chloride, bromide, iodide, acetate, dihydrogen phosphate, hydrogen sulfate, perchlorate, nitrate, and thiocyanate ions.

The corresponding absorption spectra with a 5×10^{-6} M solution of **1** in DMSO confirmed that only fluoride ion caused a distinct spectral change (Figure 1b). A characteristic new band appearing in the visible region with $\lambda_{\max} = 472$ nm can be attributed to the formation of anion [**1**]⁻, and the occurrence of proton transfer from **1** to F⁻ is dictated by the extended π -conjugation, resulting in visible spectral changes.

In another approach, we anticipated that bispyrenopyrrole **2** would exhibit a higher affinity toward F⁻ ion because the two pyrrole units might participate in the cooperative hydrogen bonding. Likewise, addition of fluoride to the DMSO solution of **2** caused a dramatic color change from greenish yellow to bright red, whereas other examined anions showed no apparent

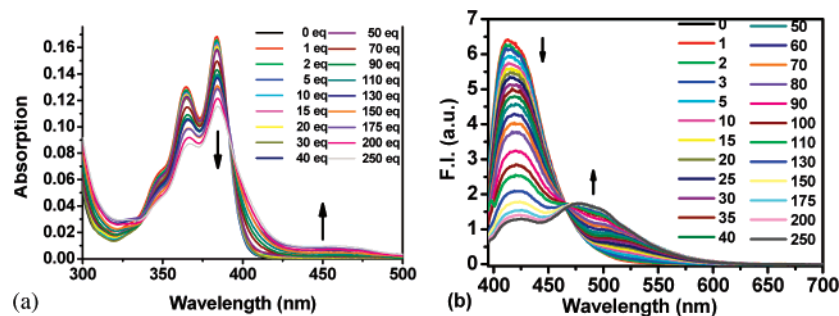


FIGURE 3. (a) Absorption titration curves of **1** (5×10^{-6} M) in CH_3CN and (b) fluorescence titration curves upon incremental addition of F^- ion (1×10^{-2} M as the Bu_4N^+ salt) in CH_3CN . $\lambda_{\text{ex}} \approx 384$ nm.

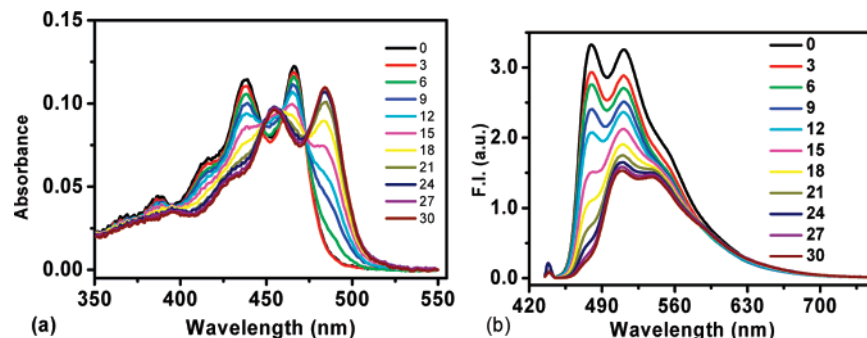


FIGURE 4. (a) Absorption titration curves of receptor **2** (5×10^{-6} M in CH_3CN). (b) Fluorescence titration curves for **2** (5×10^{-6} M in CH_3CN) upon incremental additions (0–30 equiv) of F^- ion (1×10^{-2} M as the Bu_4N^+ salt in CH_3CN). $\lambda_{\text{max}} \approx 440$ nm.

effect (Figure 2). In the UV–vis absorption spectra, growth of a new band at $\lambda_{\text{max}} = 522$ nm was prominent upon addition of F^- , though acetate and dihydrogen phosphate ions also induced slight spectral changes (see the Supporting Information).

Compounds 1 and 2 with Fluoride Ion in CH_3CN . Unlike in DMSO solution, the absorption titration of **1** against F^- in acetonitrile caused negligible spectral changes (Figure 3a). A little growth of the new absorption band at ~ 450 nm was observed only when the F^- ion was added in very large amounts (e.g., >200 equiv). As expected, the proton abstraction of **1**, in the ground state, by F^- ion appeared to be more difficult in acetonitrile than in DMSO with high polarity. However, as depicted in Figure 3b, remarkable changes of the emission were observed during the F^- titration. Upon exciting at 384 nm, which is the absorption peak of **1** in acetonitrile, the intensity of the characteristic emission maximum at 404 nm gradually decreased with concomitant growth of a new emission band at $\lambda_{\text{max}} = 479$ nm upon incremental addition of F^- . An isoemissive point was observed at 470 nm, and the stoichiometry was confirmed to be 1:1 from the Job's plot (see the Supporting Information).

The association constant in CH_3CN solution was deduced to be $K_{\text{ass}} = 2 \times 10^3 \text{ M}^{-1}$, using nonlinear least-squares treatment of fluorescence titration¹⁰ (see the Supporting Information).

The UV–vis and fluorescence titrations of sensor **2** with F^- in acetonitrile are shown in Figure 4. In contrast to negligible changes of absorption spectra in **1** (Figure 3a), the vibronic peaks at 438 and 466 nm ascribed to the free sensor **2** were significantly red-shifted upon F^- titration (Figure 4a), indicating that sensor **2** undergoes ground-state proton transfer in CH_3CN . The excitation at 440 nm led to the gradual growth of a new emission band maximized at 508 nm, accompanied by diminution of the ~ 470 -nm emission for the free sensor **2**. On the basis of 1:1 stoichiometry, the nonlinear least-squares curve fitting¹⁰ gave an association constant of $2 \times 10^4 \text{ M}^{-1}$ (see the Supporting Information). Note that this value is derived under the assumption that each formation of the **2**·fluoride hydrogen-bonded complex leads to a subsequent deprotonation, which is reasonable for the case of sensor **2** at >1 equiv fluoride ion concentration. Moreover, this value is larger than that for **1** with fluoride ion by 1 order of magnitude.

Mechanistic Study. The high electronegativity and basicity of F^- ion may be accounted for by its selectivity, among various anions including Cl^- , Br^- , I^- , AcO^- , H_2PO_4^- , HSO_4^- , ClO_4^- , NO_3^- , SCN^- , and $\text{C}_6\text{H}_5\text{CO}_2^-$, on hydrogen bonding with receptors **1** and **2**. The $\text{p}K_{\text{a}}$ in acetonitrile/ H_2O (4:1, v/v) was

(7) (a) Miyaji, H.; An, D.; Sessler, J. L. *Supramol. Chem.* **2001**, *13*, 661–669. (b) Sessler, J. L.; Maeda, H.; Mizuno, T.; Lynch, V. M.; Furuta, H. *J. Am. Chem. Soc.* **2002**, *124*, 13474–13479. (c) Anzenbacher, P., Jr.; Tyson, D. S.; Jursíková, K.; Castellano, F. N. *J. Am. Chem. Soc.* **2002**, *124*, 6232–6233. (d) Vega, I. E. D.; Camiolo, S.; Gale, P. A.; Hursthouse, M. B.; Light, M. E. *Chem. Commun.* **2003**, 1686–1687. (e) Sessler, J. L.; An, D.; Cho, W.-S.; Lynch, V. *Angew. Chem., Int. Ed.* **2003**, *42*, 2278–2281. (f) Aldakov, D.; Anzenbacher, P., Jr. *Chem. Commun.* **2003**, 1394–1395. (g) Curiel, D.; Cowley, A.; Beer, P. D. *Chem. Commun.* **2005**, 236–238. (h) Lee, C.-H.; Lee, J.-S.; Na, H.-K.; Yoon, D.-W.; Miyaji, H.; Cho, W.-S.; Sessler, J. L. *J. Org. Chem.* **2005**, *70*, 2067–2074. (i) Panda, P. K.; Lee, C.-H. *J. Org. Chem.* **2005**, *70*, 3148–3156. (j) Evans, L. S.; Gale, P. A.; Light, M. E.; Quesada, R. *Chem. Commun.* **2006**, 9, 965–967. (k) Sessler, J. L.; Cho, D.-G.; Lynch, V. *J. Am. Chem. Soc.* **2006**, *128*, 16518–16519. (l) Lu, S.-H.; Selvi, S.; Fang, J.-M. *J. Org. Chem.* **2007**, *72*, 117–122.

(8) (a) Miyaji, H.; Sessler, J. L.; Bleasdale, E. R.; Gale, P. A. *Chem. Commun.* **1999**, 1723–1724. (b) Anzenbacher, P., Jr.; Jursíková, K.; Sessler, J. L. *J. Am. Chem. Soc.* **2000**, *122*, 9350–9351. (c) Pohl, R.; Aldakov, D.; Kubát, P.; Jursíková, K.; Marquez, M.; Anzenbacher, P., Jr. *Chem. Commun.* **2004**, 1282–1283.

(9) Selvi, S.; Pu, S.-C.; Cheng, Y.-M.; Fang, J.-M.; Chou, P.-T. *J. Org. Chem.* **2004**, *69*, 6674–6678.

(10) Connors, K. A. *Binding Constants*; Wiley: New York, 1987.

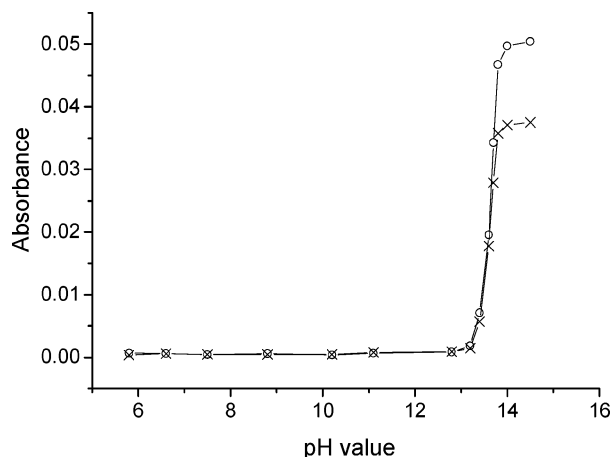


FIGURE 5. The absorbance of **1** (○, monitored at 450 nm) and **2** (×, monitored at 520 nm) in CH₃CN/H₂O (4:1, v/v) as a function of pH. Accordingly, pK_a was determined to be ~13.7 and 13.5 for **1** and **2**, respectively.

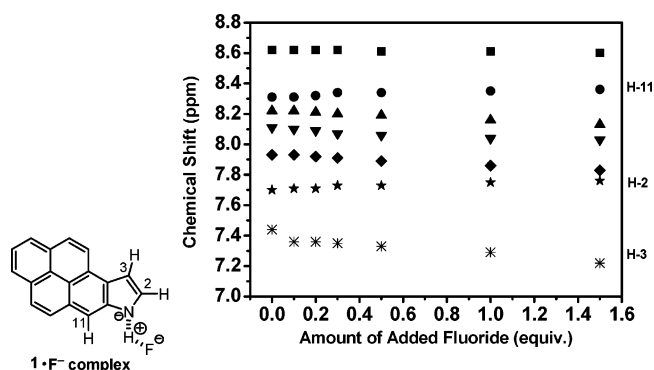


FIGURE 6. Chemical-shift changes referring to the ¹H NMR titration spectra of pyrenopyrrole **1** (5 × 10⁻³ M) with fluoride ion (as the Bu₄N⁺ salt) in CD₃CN solution (see Figure S3 in the Supporting Information). From top to bottom: (●) H11, (★) H2, and (*) H3.

determined to be ~13.7 and 13.5 for **1** and **2**, respectively (Figure 5). Due to the high pK_a value (~13.7) of **1**, the initial addition of fluoride ion (<200 equiv) to compound **1** in acetonitrile did not induce any distinct shift in the absorption maxima (~384 nm) (Figure 3a). This result indicated that sensor **1** likely bound with fluoride as an incipient hydrogen-bonded complex in the ground state at this stage.

The hydrogen-bonding interaction between F⁻ and **1** in CD₃CN was then investigated by ¹H NMR titration (Figure 6). The NH proton signal showed a continuous downfield shift as well as a decrease in intensity with increasing F⁻ concentrations. However, broadening of this peak made it impossible to follow the signal after the addition of 1 equiv of F⁻. There are two possible effects responsible for the chemical-shift changes in ¹H NMR spectra upon NH–fluoride hydrogen bond complex-

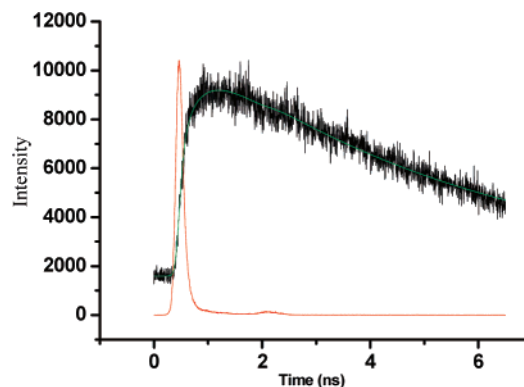


FIGURE 7. (Black) The time-dependent fluorescence of **1** in acetonitrile in the presence of fluoride ion (250 equiv) monitored at 560 nm [$\tau_1 = 305$ ps (rise) and $\tau_2 = 5.3$ ns (decay), $R^2 = 1.055$]. The excitation wavelength is 385 nm. (Red) The instrument response function monitored at the scattered light of 560 nm (fwhm ~45 ps, see the Experimental Section).

ation:¹¹ (i) the through-bond effects, which would increase the electron density to cause upfield shifts, and (ii) the through-space effects, which would polarize the C–H bond proximal to the NH–fluoride moiety to induce a downfield shift due to the partial positive charge developed on the *N*-proton. In the titration spectra (see Figure S3 in the Supporting Information), the formation of the **1**·F⁻ hydrogen-bonded complex caused a through-bond shielding effect, giving particularly the distinct upfield shift of H-3 (Figure 6). In contrast, the partial positive charge created at the *N*-proton caused somewhat through-space deshielding effects on the proximal H-2 and H-11. When more F⁻ ions were added, deprotonation might occur subsequently to form the [1]⁻ anion, so that the through-bond effect would predominate over the through-space effect.^{11b,c} As a consequence, the upfield shifts of H-3 continued, whereas the deshielding effects on H-2 and H-11 diminished. Another NMR titration experiment of **1** with F⁻ was similarly conducted in DMSO-*d*₆ solution. The occurrence of a triplet ($J = 119.6$ Hz) at δ 16.1 clearly indicated the formation of the [FHF]⁻ species (see the Supporting Information).^{11c} Thus, addition of excess F⁻ did promote the deprotonation of NH to form the [1]⁻ anion, which was stabilized in the highly polar solvent of DMSO.

Hydrogen bonding of **1** with F⁻ revealed anomalously large Stokes shifts of 75 nm (from λ_{\max} 404 to 479 nm) in its emission spectra (Figure 3b). In another approach, the titration of **1** with OH⁻ ion in CH₃CN solution also formed an anion species of **1** to show similar fluorescence changes (see the Supporting Information), supporting that the 479 nm emission originates from an anion emission of **1**. Since the excitation spectrum monitored at the anion emission (>470 nm) gives a spectral profile identical with the absorption spectrum of the hydrogen-bonded complex, the [1]⁻ anion mainly forms in the electronically excited state. It should be noted that, for a strong hydrogen-bonding configuration with polar solvent molecules, the intermolecular excited-state proton transfer takes place for several indole type chromophores,¹² leading to an ion pair formation. Thus, it is reasonable to expect an increase of acidity of NH upon electronic excitation in the hydrogen-bonded **1**·F⁻ complex, such that proton transfer might take place from **1** to

(11) (a) Boiocchi, M.; Boca, L. D.; Esteban-Gómez, D.; Fabbrizzi, L.; Licchelli, M.; Manzani, E. *J. Am. Chem. Soc.* **2004**, *126*, 16507–16514. (b) Peng, X.; Wu, Y.; Fan, J.; Tian, M.; Han, K. *J. Org. Chem.* **2005**, *70*, 10524–10531. (c) Esteban-Gómez, D.; Fabbrizzi, L.; Licchelli, M. *J. Org. Chem.* **2005**, *70*, 5717–5720. (d) Amendola, V.; Esteban-Gómez, D.; Fabbrizzi, L.; Licchelli, M. *Acc. Chem. Res.* **2006**, *39*, 343–353. (e) Kang, S. O.; Powell, D.; Day, V. W.; Bowman-James, K. *Angew. Chem., Int. Ed.* **2006**, *45*, 1921–1925. (f) Wu, C.-Y.; Chen, M.-S.; Lin, C.-A.; Lin, S.-C.; Sun, S.-S. *Chem. Eur. J.* **2006**, *12*, 2263–2269. (g) Black, C. B.; Andrioletti, B.; Try, A. C.; Ruiperez, C.; Sessler, J. L. *J. Am. Chem. Soc.* **1999**, *121*, 10438–10439.

(12) Yu, H.-T.; Colucci, W. J.; McLaughlin, M. L.; Barkley, M. D. *J. Am. Chem. Soc.* **1992**, *114*, 8449–8454.

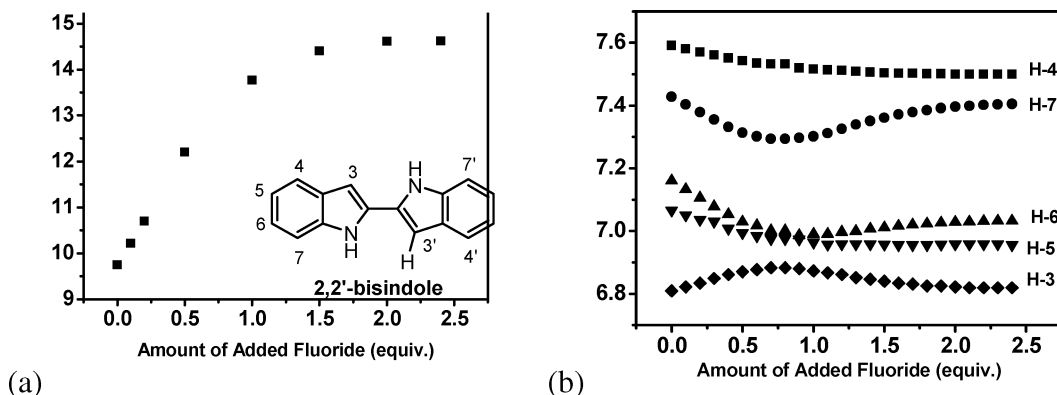


FIGURE 8. Chemical-shift changes referring to the ^1H NMR titration spectra of 2,2'-bisindole **3** (5×10^{-3} M) with fluoride ion (as the Bu_4N^+ salt) in CD_3CN solution (see Figure S9 in the Supporting Information): (a) chemical-shift changes of NH induced by addition of fluoride ions and (b), from top to bottom, chemical-shift changes of H4 (■), H7 (●), H6 (▲), H5 (▼), and H3 (◆).

F^- even in CH_3CN solution to account for the anion $[\mathbf{1}]^-$ emission at $\lambda_{\text{max}} \approx 479$ nm.

Further support was rendered by the dynamic approaches. During the fluoride ion titration of compound **1**, the time-resolved single photon counting experiment resolved a rise component of ~ 300 ps upon monitoring at the 474 nm emission band (Figure 7), suggesting a finite time required for the solvation of the $[\mathbf{1}]^-$ anion and proton species.

In the case of sensor **2**, insufficient solubility in CD_3CN prohibited the ^1H NMR study. In an attempt to gain further insights into the associated mechanism, we thus synthesized 2,2'-bisindole (**3**)¹³ possessing functional similarity with **2**, and carried out its ^1H NMR titration in CD_3CN at 25°C (see Figure S9 in the Supporting Information). Interestingly, the characteristic protons of **3** shifted in a reversed manner (Figure 8b), in comparison with those of **1**. At the early stage of titration with F^- (< 1 equiv), the H-3 ($3'$) in compound **3** showed downfield shifts rather than the upfield shifts of H-3 in **1**. Conversely, H-7 ($7'$) in **3** shifted to upfield, whereas the corresponding H-11 in **1** shifted to downfield.

The two aromatic rings in bisindole **3** (and bis-pyrenoidole **2**) likely existed in twisted conformations as those usually observed in biphenyl systems, and the anti form with two N–H's pointing to opposite directions might be favored over the syn form in the twisted conformation (Figure 9). Upon addition of F^- , the $3 \cdot \text{F}^-$ hydrogen-bonded complex might form with a partial positive charge developed at the N-proton, as evidence of the continuous downfield shifts of the NH signal in the ^1H NMR spectra (Figure 8a) and the changes of fluoride signal in the ^{19}F NMR spectra during titration (see Figure S10 in the Supporting Information). As the $\text{C}_3\text{--H}$ (or $\text{C}_3'\text{--H}$) is close to the polarized NH on the adjacent indole ring, the through-space effect would induce a downfield shift. In contrast, the upfield shifts of H-4 ($4'$) and H-7 ($7'$) might be attributable to the predominant through-bond effects. Further addition of excess F^- ions would facilitate the formation of $[\mathbf{3}]^-$ anion, which might exist in the syn conformation with charge delocalization between the two nitrogen atoms. As a consequence, the through-space effect due to polarization would diminish. The formation of HF_2^- at the late stage of titration with excess F^- was also identified by the occurrence of a triplet at δ 16.1 ($J = 119.6$ Hz) in $\text{DMSO-}d_6$ solution (see the Supporting Information). Due

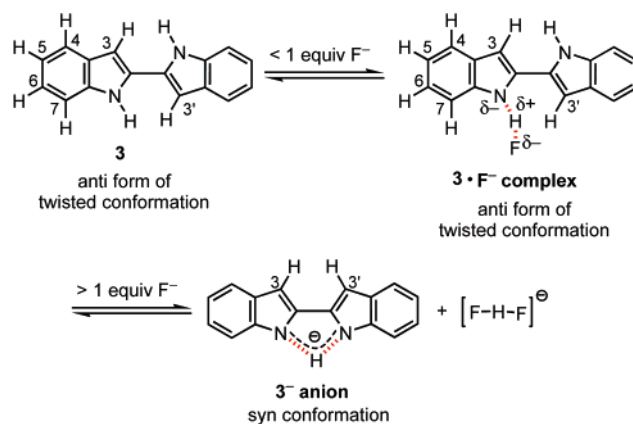


FIGURE 9. Proposed interaction modes of 2,2'-bisindole with fluoride ions.

to the charge delocalization, thermodynamically, the anion species of **2** is expected to be more stable than that of **1**. This rationalizes the result that deprotonation of sensor **1** by fluoride ions is difficult in acetonitrile in the ground state, but fluoride can easily induce the deprotonation of sensor **2** (vide supra).

Supplementary support of the above proposed structural variation is also given by a theoretical approach (see the Experimental Section). As listed in the Supporting Information (Table S1), the molecular calculations of bis-pyrenoidole **2** revealed that the anti form of the twisted conformation is favored by ~ 2 kcal/mol over the syn form. When one NH binds with F^- in the anti form, the $\text{C}_3\text{--H}$ ($\text{C}_3'\text{--H}$) bond is somewhat polarized with an extended length (Table S1), a result in agreement with the through-space effect causing the downfield shifts of the counterpart in the $3 \cdot \text{F}^-$ hydrogen-bonded complex (Figure 9). Moreover, the molecular calculation also supports the preferable existence of bis-pyrenopyrrole anion in the syn conformation, similar to that depicted for $[\mathbf{3}]^-$, with a stabilization energy of ~ 8.6 kcal/mol.

Conclusion

In conclusion, we have successfully employed pyrenopyrrole **1** and its dimeric derivative **2** as the selective and sensitive sensors for fluoride ion. The selectivity for F^- among various anions may be accounted for by the high electronegativity and basicity of the F^- ion. These two molecular sensors provide both colorimetric and fluorescent detections in the visible region

(13) Koradin, C.; Dohle, W.; Rodriguez, A. L.; Schmid, B.; Knochel, P. *Tetrahedron*, **2003**, *59*, 1571–1587.

with the advantages for real-time and on-site application. We thus demonstrate for the first time the use of parent pyrenopyrroles as chemosensors. Since pyrene has been extensively used in signal transduction,¹⁴ the general strategy can be applied on pyrenopyrroles. Taking into account the advantage of versatile chemistry on nitrogen-containing aromatic compounds,¹⁵ the structural elaboration of pyrenopyrroles, including those are compatible in aqueous systems, should be feasible.⁹

We have also investigated the interaction modes by detailed analyses of the NMR and dynamic fluorescence spectra. The initial interaction mode of **1** with F⁻ in CH₃CN can be understood as the hydrogen-bonded complex in the ground state that shows little absorption spectral change, and proton transfer in the excited state that causes a remarkable bathochromic fluorescence change. Bis(pyrenopyrrole) **2** undergoes a ground state deprotonation by F⁻ even in CH₃CN, though both **1** and **2** undergo ground state deprotonations in the highly polar solvent of DMSO.

Experimental Section

The preparation and characterization of compounds **1** and **2** have been previously reported.⁹

UV–Vis and Fluorescence Titrations. The stock solutions of **1** and **2** (5×10^{-6} M) were prepared by using spectroscopic grade CH₃CN or Me₂SO. The Bu₄NF solution was prepared as 1×10^{-2} M. The solution containing compound **1** or **2** (2 mL of stock solution) was placed in a quartz cell (1 cm width), and the Bu₄NF solution was introduced in an incremental fashion. Their corre-

sponding UV–vis and fluorescence spectra were recorded at 298 K. Nonlinear regression analyses were used to determine the association constants.

Time-Correlated Single Photon Counting Experiment. The setup of picosecond dynamical measurements consisted of a femtosecond Ti-Sapphire oscillator (82 MHz, Spectra Physics). The fundamental train of pulses was pulse-selected (Neos, model N17389) to reduce its repetition rate to typically 0.8–8 MHz, and then used to produce second harmonics (375–425 nm) as an excitation light source. An Edinburgh OB 900-L time-correlated single photon counting system was used as a detecting system, rendering a temporal resolution of ~15 ps. In addition, a Berek's variable waveplate was placed in the pump beam path to ensure that the polarization of the pump laser was set at the magic angle (54.7°) with respect to that of the probe laser (or detecting system) to eliminate the fluorescence anisotropy.

¹H NMR Titration. ¹H NMR spectra were measured on 400 MHz NMR spectrometers. A solution of **1** (or **3**) in CD₃CN (or DMSO-*d*₆) was prepared (5×10^{-3} M), and a 0.4-mL portion was transferred to a 5-mm NMR tube. A small aliquot of Bu₄NF in CD₃CN (or DMSO-*d*₆) was introduced in an incremental fashion, and their corresponding spectra were recorded.

Molecular Calculations. All calculations were done with Turbomole 5.8 by the hybrid DFT functional, B3LYP and SVP basis set.^{16,17} The B3LYP functional in Turbomole was different from the same functional in the Gaussian program due to using the correlation functional VWN V and not VWN III. All minima were checked by the script aoforce to confirm the number of imaginary frequencies was zero.¹⁸ The spherical grid size and the SCF convergence criteria were set to 4 and 7, respectively. The magnetic shielding was calculated by the script mpshift in the Turbomole package.¹⁹

Acknowledgment. We thank Prof. Jye-Shane Yang (Department of Chemistry, National Taiwan University) for helpful discussion and the National Science Council for financial support.

Supporting Information Available: Synthetic procedures, absorption, fluorescence, ¹H and ¹⁹F NMR titration curves, Job's plots and isotherms. This material is available free of charge via the Internet at <http://pubs.acs.org>.

JO070169W

(16) Ahlrichs, R.; Bar, M.; Haser, M.; Horn, H.; Kolmel, C. *Chem. Phys. Lett.* **1989**, *162*, 165–169.

(17) Treutler, O.; Ahlrichs, R. *J. Chem. Phys.* **1995**, *102*, 346–354.

(18) Deglmann, P.; Furche, F. *J. Chem. Phys.* **2002**, *117*, 9535–9538.

(19) Haser, M.; Ahlrichs, R.; Baron, H. P.; Weis, P.; Horn, H. *Theor. Chim. Acta* **1992**, *83*, 455–470.

(14) For reviews, see: (a) Dorjpalam, N.; Toda, M.; Itoh, H.; Hamada, F. *J. Inclusion Phenom. Macrocyclic Chem.* **2004**, *50*, 79–85. (b) Ueno, A. *Supramol. Sci.* **1996**, *3*, 31–36. For recent examples, see: (c) Fujimoto, K.; Muto, Y.; Inouye, M. *Chem. Commun.* **2005**, 4780–4782. (d) Cho, H. K.; Lee, D. H.; Hong, J.-I. *Chem. Commun.* **2005**, 1690–1692. (e) Lee, J. Y.; Kim, S. K.; Jung, J. H.; Kim, J. S. *J. Org. Chem.* **2005**, *70*, 1463–1466. (f) Kuo, L.-J.; Liao, J.-H.; Chen, C.-T.; Huang, C.-H.; Chen, C.-S.; Fang, J.-M. *Org. Lett.* **2003**, *5*, 1821–1824 and the references cited therein. (g) Liao, J.-H.; Chen, C.-T.; Fang, J.-M. *Org. Lett.* **2002**, *4*, 561–564. (h) Kim, J. S.; Shon, O. J.; Rim, J. A.; Kim, S. K.; Yoon, J. *J. Org. Chem.* **2002**, *67*, 2348–2351. (i) Ohtani, Y.; Yamana, K.; Nakano, H. *Nucleic Acids Res.* **2002**, *2* (Suppl.), 169–170. (j) Yang, J.-S.; Lin, C.-S.; Hwang, C.-Y. *Org. Lett.* **2001**, *3*, 889–892. (k) Smalley, M. K.; Silverman, S. K. *Nucleic Acids Res.* **2006**, *34*, 152–166. (l) Brea, R. J.; Va'zquez, E.; Mosquera, M.; Castedo, L.; Granja, J. R. *J. Am. Chem. Soc.* **2007**, *129*, 1653–1657.

(15) (a) Eisenstadt, E. *ACS Symp. Ser.* **1985**, *283*, 327–340. (b) Snieckus, V. *Chem. Rev.* **1990**, *90*, 879–933. (c) Hartung, C. G.; Snieckus, V. *Mod. Arene Chem.* **2002**, 330–367.